

Document downloaded from:

<http://hdl.handle.net/10251/102305>

This paper must be cited as:



The final publication is available at

<https://doi.org/10.1021/acs.bioconjchem.6b00624>

Copyright American Chemical Society

Additional Information

1

2 **Improved Performance of DNA Microarray**

3 **Multiplex Hybridization Using Probes Anchored**

4 **at Several Points by Thiol-Ene or Thiol-Yne**

5 **Coupling Chemistry**

6 Maria-Jose Bañuls^a, Pilar Jiménez-Meneses^a, Albert Meyer^b, Jean-Jacques Vasseur^b,
7 François Morvan^{b*}, Jorge Escorihuela^{a†}, Rosa Puchades^a, Ángel Maquieira^{a*}

8 *^aInteruniversity Research Institute for Molecular Recognition and Technological*
9 *Development (IDM), Chemistry Department, Universitat Politècnica de València,*
10 *Camino de Vera s/n, 46022 Valencia, Spain*

11 *amaquieira@gim.upv.es

12 *^bInstitut des Biomolécules Max Mousseron (IBMM), UMR 5247 CNRS, Université de*
13 *Montpellier, ENSCM, place Eugène Bataillon, CC1704, 34095 Montpellier Cedex 5,*
14 *France.*

15 *francois.morvan@umontpellier.fr

16 *[†]J. Escorihuela present address is Laboratory for Organic Chemistry, Wageningen*
17 *University, Dreijenplein 8, 6703HB Wageningen, The Netherlands.*

18 **ABSTRACT**

19 Nucleic acid microarray-based assay technology has shown lacks in reproducibility,
20 reliability and analytical sensitivity. Here, a new strategy of probe attachment modes for
21 silicon-based materials is built up. Thus, hybridization ability is enhanced combining
22 thiol-ene or thiol-yne click chemistry reactions, with a multi-point attachment of
23 polythiolated probes. The viability and performance of this approach was demonstrated
24 specifically determining *Salmonella* PCR products up to 20 pM sensitivity level.

25

26 **INTRODUCTION**

1 The development of high-performance methods for the sensitive and selective detection
2 of DNA and RNA targets has become a key point in biomedical and clinical studies,¹
3 agricultural, food and environmental fields.²⁻⁴ Among the working techniques,
4 microarraying emerges as a tool showing parallel and high throughput assay capabilities.⁵
5 However, both clinical and analytical metrics produced by microarray-based assay
6 technology have recognized lacks in reproducibility, reliability and analytical sensitivity.⁶
7 Most of these drawbacks are attributed to poor probe attachment and solid-liquid interface
8 control.⁷

9 Indeed, the success of microarray-based techniques depends on the good accessibility and
10 functionality of the surface-bound probes, which closely relates to the chemistry of
11 attachment (support nature, probe orientation, probe density, reproducibility).^{8,9} Many
12 work have been developed in this field involving passive immobilization by adsorption
13 forces,¹⁰ electrostatic interactions,¹¹ affinity reactions¹² and covalent bonding.¹³⁻¹⁵ But,
14 nowadays there is still a need for better attachment modes providing high performance in
15 the developed microarray; specially regarding sensitivity and selectivity.

16 Generally, covalent binding is the preferred approach for the probe attachment, because
17 it provides good stability and high binding strength, controlling also orientation and
18 density of probes. However, it has several drawbacks as the need of linker molecules,
19 slow procedures and crowding effects.⁷

20 Despite the many methods described for microarray probe covalent anchoring; the most
21 interesting reported approaches to overcome the abovementioned drawbacks, are those
22 based on click chemistry reactions.¹⁶ Thiol-ene^{17,18} and thiol-yne^{19,20} coupling chemistries
23 belong to this family, which are characterized by orthogonality, high yields,
24 regioselectivity, compatibility with aqueous media, mild reaction conditions, use of
25 benign catalysts and solvents, and high reaction rates. The good performance of these
26 coupling chemistries made them useful for many applications such as in polymers,
27 dendrimers, bioconjugation and surface photografting.²¹⁻²³

28 However, few examples can be found employing these click reactions for microarray
29 fabrication.²⁴⁻³⁰ Regarding thiol-ene coupling, the most interesting contributions are those
30 by Waldmann and colleagues,²⁷⁻³⁰ but they are basically centered in the use of
31 farnesylated proteins to induce surface photopatterning. Recently, we reported the use of
32 thiol-ene^{31,32} and thiol-yne³³ click reactions to couple monothiolated oligonucleotides
33 onto alkenylated or alkynylated silicon-based surfaces in a direct, clean and quick way.

1 The obtained DNA microarrays detected bacterial PCR products with high sensitivity and
2 selectivity.

3 Aiming to improve the performance of the fabricated microarrays even more, several
4 important technical issues still remain challenging. These include reducing surface effects
5 such as steric hindrance and electrostatic interactions and controlled arranging of the
6 capture biomolecules in an oriented manner, providing a solution-phase-like environment
7 for biorecognition.

8 Recently, Morvan and colleagues³⁴ reported rapid genotyping of hepatitis C virus using
9 polythiolated probes. These probes developed in this study displayed an increased
10 sensitivity in both in vitro ELOSA on maleimide activated plates and electrochemical
11 assays on gold electrodes.

12 Here, analogous polythiolated probes are used for the first time on silicon-based materials
13 by thiol-ene and thiol-yne click chemistries to tether the nucleic acids in an optimal
14 manner. The method should provide quick, fast, clean, environmentally friendly and
15 optimally oriented probe immobilization. Thus, a new generation of microarrays is
16 constructed where hybridization ability is enhanced due to the combination of click
17 chemistry orthogonality and multipoint surface attachment of polythiols. In this way, the
18 less hydrophobic surfaces can reach similar performance than the more hydrophobic ones
19 just by multi-point attachment of the probe. Sensitivity and selectivity for real samples
20 are evaluated by detecting *Salmonella* and *Campylobacter* PCR products.

21

22 **RESULTS AND DISCUSSION**

23 The process of DNA hybridization at surfaces is a critical part of nucleic acid-based array
24 technology and fundamental understanding of this process under relevant conditions for
25 actual assays is currently very challenging. Thus, controlling probe density on substrates
26 to further optimize probe-target binding kinetics is important.

27 This will allow to develop new microarray surfaces with better performance within
28 complex media. For the first time, a double control on the microarray performance is
29 exerted by combining surface hydrophobicity tuning and multi-point probe attachment.
30 The modulation of the hybridization capability allows detecting the presence of bacterial
31 DNA and, at the same time, in the same chip, quantifying the microorganism level.

32 Polythiolated oligonucleotides with and without Cy5 dye were obtained on a DNA
33 synthesizer according to standard phosphoramidite chemistry, starting from nucleoside

1 or Cy5 solid supports. After elongation of the sequence, the thiol functions were
2 introduced with the same chemistry allowing a straightforward obtaining of mono and
3 polythiolated oligonucleotides.³⁴ The crucial point was to remove the cyanoethyl
4 protecting group of the phosphate before deprotection of the thiol functions. Indeed the
5 acrylonitrile formed during classic ammonia treatment strongly reacts with a thiol leading
6 to further unreactive thiol-cyanoethyl. For that purpose, the solid-supported thiolated
7 oligonucleotides were firstly treated with piperidine allowing the selective removal of the
8 cyanoethyl groups. Secondly, after washes, the ammonia treatment was applied for the
9 release from the solid support and the deprotection of the oligonucleotide. Note that the
10 thiol function rapidly oxidized due to oxygen dissolved in solvent leading to a disulfide
11 bridge that should be reduced before immobilization of the mono and polythiolated
12 oligonucleotides on a surface.

13

14 **Studies in microarray format.** Before organosilanization, the silicon oxide chips were
15 activated employing a UV-ozone cleaning system. Different exposition times were tried,
16 and water contact angles measured. Finally, an activation time of 7 min was set (Figure
17 S2, Supporting Information.). Immediately after activation, the chips were immersed into
18 a solution of 2% organosilane in toluene for 2 h, under mild stirring. In the case of alkenyl
19 surfaces, two organosilanes were tried showing similar results, allyltrimethoxysilane and
20 vinyltrimethoxysilane, we decided to use vinyltrimethoxysilane for further studies. In the
21 case of alkynyl derivatization, after silanization, the chips were treated with 2%
22 propargylamine in toluene for 4 h. The success in the surface functionalization was
23 evaluated by measuring the water contact angle (Figure 1 and Table S2, Supporting
24 Information).

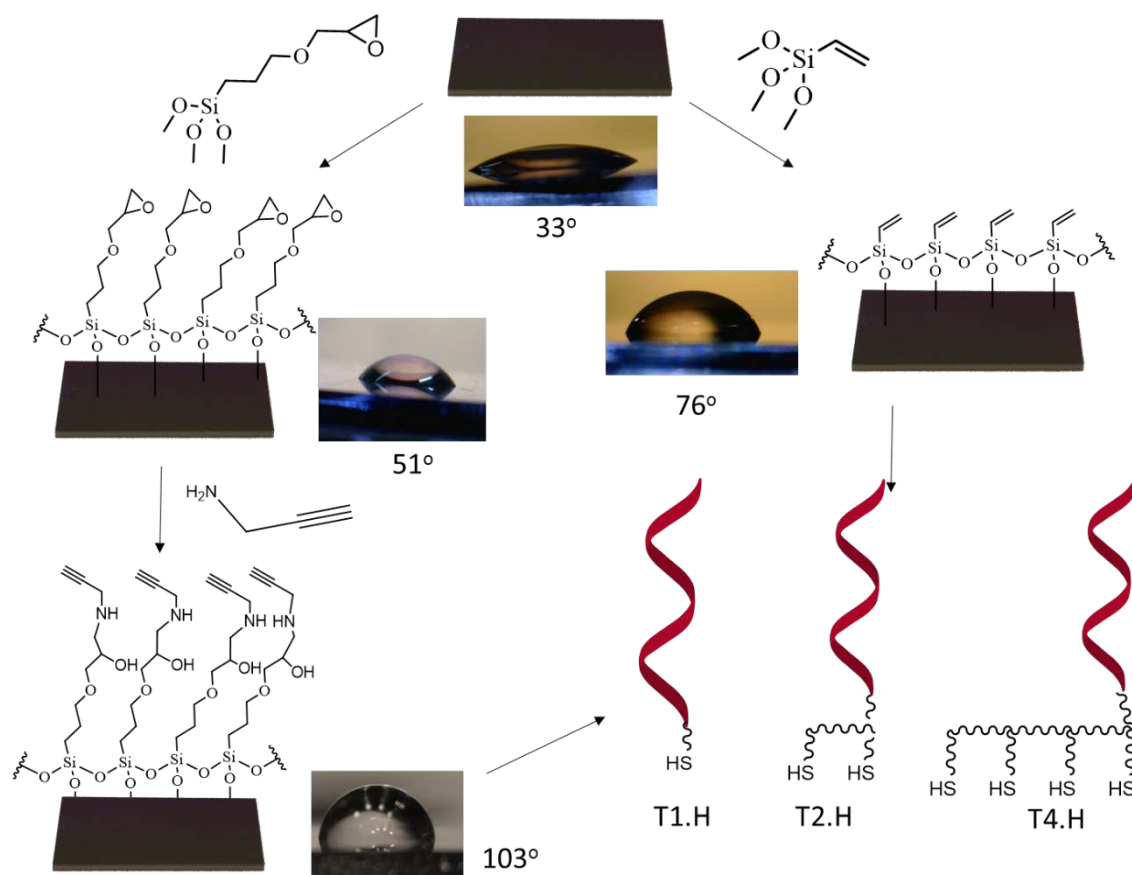
25 In this way, alkenylated and alkynylated surfaces were ready to immobilize mono, di and
26 tetrathiolated oligonucleotide probes using thiol-ene and thiol-yne coupling chemistries.

27

28

29

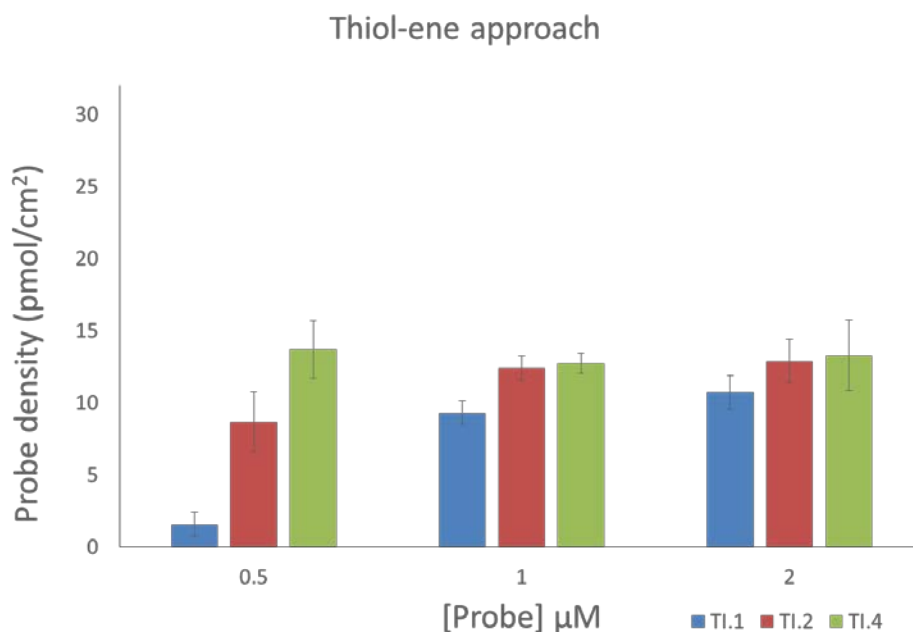
30



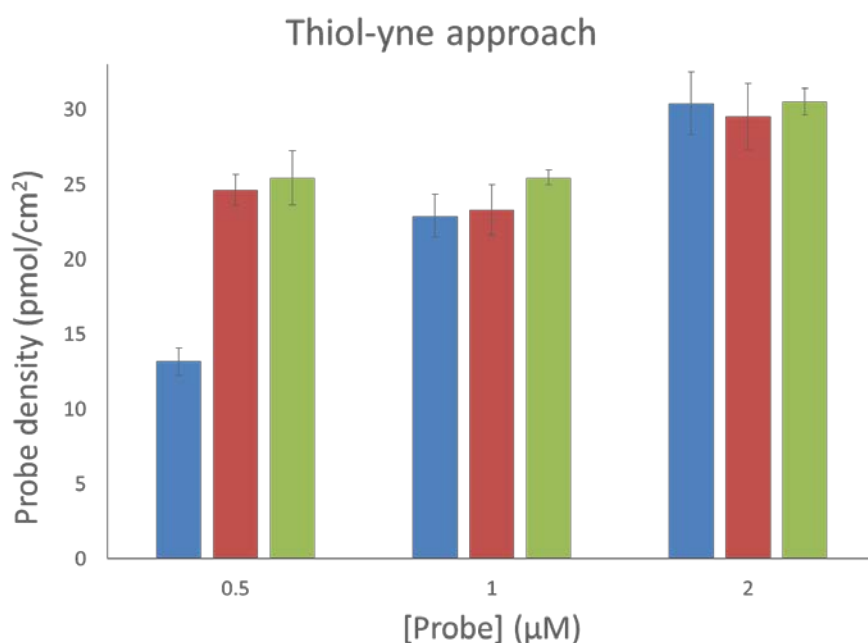
1
 2 **Figure 1.** Scheme showing the different functionalization approaches providing alkyne and alkene ended
 3 surfaces, to attach mono-, di- and tetra-thiolated oligonucleotides. Water contact angles were measured for
 4 each surface to assess the progress in the derivatization

5
 6 Firstly, the mono and polythiolated probes were compared regarding their immobilization
 7 capabilities. For this, an array was created onto the functionalized surfaces containing
 8 T1.I, T2.I and T4.I at three different concentrations (0.5, 1 and 2 μM). T1.I stands for the
 9 monothiolated probe, while T2.I and T4.I correspond to the di- and tetra-thiolated probes,
 10 respectively. All of them bore a fluorescence tag. Three replicas of each microarray were
 11 done and, after irradiating at 365 nm and washing, the fluorescence was registered and
 12 compared. The results are summarized in Figure 2, where immobilized probe density is
 13 plotted against the spotted probe concentration for each attachment approach. The amount
 14 of immobilized probe was calculated from the decrease in the fluorescence signal after
 15 washings, and considering the printed volume (40 nl) and the area of the spots.
 16 The conclusion extracted for alkenyl-terminated surfaces was that polythiolated probes
 17 immobilized more effectively on the surface than the monothiolated ones when the probes
 18 were spotted at low concentration (0.5 and 1 μM). For alkyne-ended surfaces, the three
 19 probes showed similar immobilization behavior, with no significant differences between

1 them for concentration of 1 and 2 μM , while at 0.5 μM concentration, the monothiolated
2 probe exhibited a much lower density of immobilization. In all cases, the amount of
3 immobilized probes was higher for thiol-yne coupling chemistry ($30.52 \text{ pmol}/\text{cm}^2$) than
4 for thiol-ene one ($13.27 \text{ pmol}/\text{cm}^2$) (Table S3, Supporting Information).



5



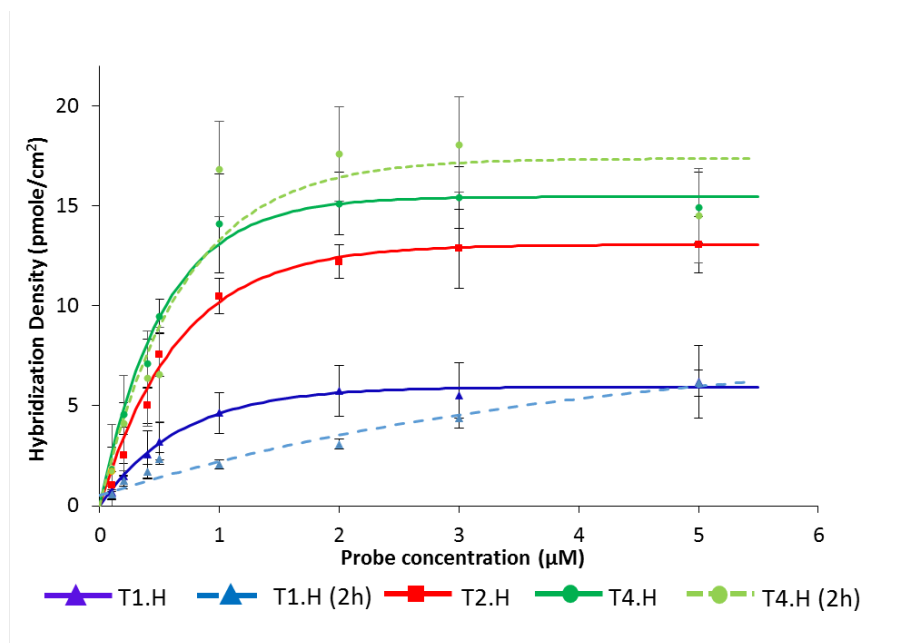
6

7

8 **Figure 2.** Immobilized probe density (pmol/cm^2) for mono (blue), di (red) and tetrathiolated (green)
9 oligonucleotides onto alkenylated (thiol-ene coupling: TEC) and alkyne-terminated (thiol-yne coupling:
10 TYC) surfaces after irradiation at 365 nm for 1h.

1 Besides, the use of tetrathiolated probes reached the maximal immobilization density
2 regardless the probe concentration used, whereas for the mono- and di-thiolated probes,
3 higher probe concentrations were needed to achieve maximum immobilization densities.
4 Experiments carried out by Raman spectroscopy and using the Ellman's test did not show
5 evidence of free thiol on the surface after the attachment. However, no conclusive result
6 were obtained. The Ellman's test was not sensitive enough to detect amounts of thiols in
7 the order of our amounts. In the Raman spectra, the presence of other bands from the
8 oligonucleotide structure overlapped the band at 2546 cm^{-1} specific for free thiols.
9 As it is known, a higher immobilization density can render less effective hybridization
10 yield.^[7] Thus, a new set of chips were functionalized and arrays of probes printed as
11 before, but now using T1.H, T2.H and T4.H. These probes were similar to T1.I, T2.I and
12 T4.I but without the fluorescent tag. Microarrays with growing concentrations of probe
13 (from 0.5 to 5 μM) were printed. After irradiation at 365 nm for 60 min, and washing, the
14 chips were hybridized with Target A 0.5 μM in SSC 1 \times for 60 min at 37 °C. The amount
15 of hybridized oligonucleotide was determined interpolating the fluorescence intensity in
16 the corresponding calibration curve (Figure S3, Supporting Information). What is
17 explained on the basis of the higher surface hydrophobicity, which reduces the contact
18 area and forces the probes to anchor the surface in a denser way.
19 The hybridization densities were higher for thiol-yne coupling chemistry than for thiol-
20 ene coupling, indicating that the highest immobilization density still allows for the
21 complementary strand to reach most of the probes, and there is not crowding effects.
22 Thus, the immobilized probe density was double in thiol-yne than in thiol-ene coupling,
23 and also the hybridization densities. However, the most important feature for our study
24 was that in thiol-ene approach, the multipoint attachment of probes improved
25 significantly the immobilization density and thus the hybridization with the
26 complementary strand (Figure 3a).
27 From the obtained data of immobilization densities for probes T1.I, T2.I and T4.I at 1 and
28 2 μM ; and referring them to the values of hybridization density, it was possible to
29 calculate the hybridization efficiency in each case. In Table 1, the estimated hybridization
30 yields are shown.
31

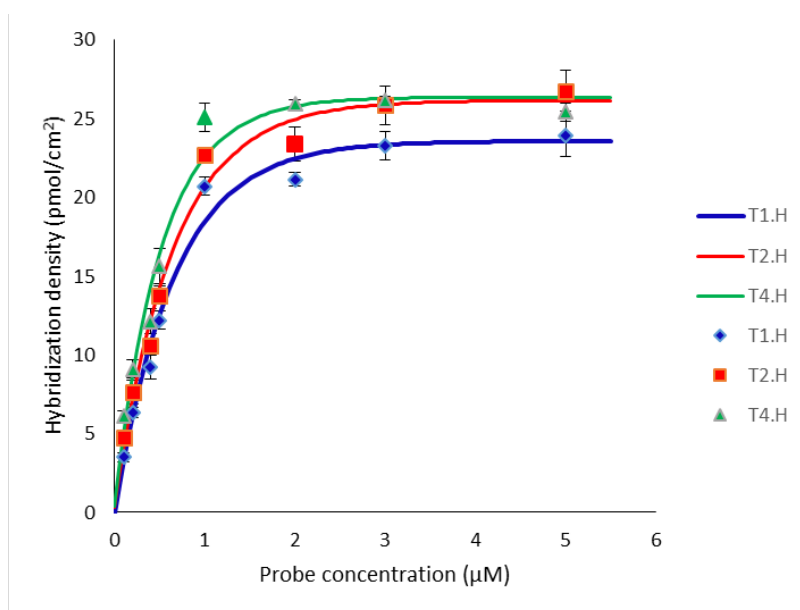
1 a)



2

3

b)



4

5 **Figure 3.** Hybridization densities obtained for Target A 0.5 µM in microarrays with growing
6 concentrations of mono- (T1.H), di- (T2.H) and tetra-thiolated (T4.H) probes attached to the surface
7 by means of a) thiol-ene coupling and b) thiol-yne coupling. In a) the dashed lines are for
8 hybridization curves obtained under similar hybridization conditions, but for TH.1 and TH.4
9 irradiated for 2 h instead of 1 h.

10

11 Regardless of the concentration of spotted probe (1 or 2 µM), the hybridization efficiency
12 increased when the number of thiols contained in the probe grew. This feature was
13 observed for both thiol-ene and thiol-yne approaches. However, it was enhanced in the
14 case of thiol-ene coupling, where the hybridization yield increased from 54% for T1.H at

1 1 μM to 85% and 100% for T2.H and T4.H, respectively. In the case of thiol-yne
 2 approach, the effect was less pronounced due to the high yields obtained in all the cases.
 3 Thus, yields changed from 90% for T1.H (1 μM) to 98 and 99% for T2.H and T4.H,
 4 respectively. Same pattern was observed at the 2 μM concentration.

5 In the case of thiol-ene coupling, longer reaction times did not lead to higher probe
 6 immobilization or better hybridization densities. Thus, irradiation times of 2 h instead of
 7 1 h provided hybridization yields very similar to that obtained for 1 h irradiation, for both
 8 TH.1 and TH.4 (Figure 3a, dashed lines)

9 When analyzing the influence of the multipoint attachment in the molecular crowding
 10 effect, higher differences between thiol-ene and thiol-yne coupling were appraised. Thus,
 11 when comparing the hybridization percentages under saturation of probe, changing from
 12 1 to 2 μM , for T1.H, meant a decrease in hybridization efficiency, which lowered from
 13 53% to 42%. This fact, although, was not noticed for T2.H and T4.H, which even
 14 increased the hybridization yields (from 85 to 96% in T2.H). T4.H kept the maximal
 15 hybridization efficiency for both probe concentrations (Table 1).

16

17 **Table 1:** Hybridization percentage referred to the immobilized density for a probe concentration of 1 and
 18 2 μM , for thiol-ene and thiol-yne approaches and using mono-, di- and tetra-thiolated probes.

19

Probe conc. (μM)	Thiol-ene approach			Thiol-yne approach		
	T1.I	T2.I	T4.I	T1.I	T2.I	T4.I
	Immobilized density (pmol/cm ²)					
1	8.7	12.4	12.9	22.9	23.3	25.5
2	13.7	12.7	13.3	30.4	29.5	30.5
	Hybridization density (pmol/cm ²)					
1	4.6	10.5	14.1	20.7	22.7	25.1
2	5.7	12.2	15.1	21.2	23.4	26.0
	Hybridization yield (%)					
1	54	85	100	90	98	99
2	42	96	100	70	79	85

20

21 The molecular crowding effect was also noticed using the monothiolated probe in thiol-
 22 yne coupling surfaces, lowering the yield from 90 to 70%, when spotted concentrations
 23 of T1.H moved from 1 to 2 μM . Di- and tetra-thiolated probes showed also a slight
 24 crowding effect. However, it was much lower than in the case of the monothiolated probe.

1 Thus, the hybridization yield decreased from 98 to 79% in T2.H, and from 99 to 85% in
2 T4.H. To assess reproducibility, the assays were done in triplicate, and repeated on
3 different days. The intrachip RSD oscillated between 5% and 12%, meanwhile interchip
4 RSD was in the range from 12% to 15%.

5 AFM and XPS studies on alkene biofunctionalized chips were also performed before and
6 after hybridization (Figures S4 and S5, Supporting Information). The results agreed with
7 that observed in the microarrays, the amount of immobilized probe was higher for di and
8 tetrathiolated probes than for monothiolated one.

9 As conclusion, the use of di- and tetra-thiolated improved the performance of the
10 hybridization, especially in the case of thiol-ene coupling surfaces or when the crowding
11 effect acted. Briefly, there are two ways to improve the performance of a microarray: to
12 focus on the surface functionalization and tune its features, or to link the probe using a
13 multipoint attachment. Both options seem to be closely related to the configuration
14 adopted by the probe once attached, which determines its bioavailability, and which is
15 influenced by the properties of the surface itself (hydrophobicity, etc) and the anchoring
16 way.

17 In order to look more deeply in the hybridization process for the different situations, a
18 complete study was done using dual polarization interferometry (DPI). In this technique,
19 the hybridization is monitored label-free in real time and thus, data about the mass surface
20 density, the change in thickness and density are obtained. This can give some light on
21 how the immobilized probes are set in each case, and the changes that they experience
22 after hybridization.

23 For that purpose, unmodified Anachips (containing two channels available for
24 measurements) were derivatized with alkenyl or alkynyl groups. Taking advantage of our
25 immobilization chemistry, the chips were functionalized with a different thiolated probe
26 on each channel, using selective irradiation through a homemade photomask. Thus, a set
27 of four chips were ready for DPI studies containing the following pairs of probes
28 immobilized in the channels: Probes T1.H vs T2.H as well as T1.H vs T4.H by thiol-ene
29 coupling chemistry and the pairs T1.H vs T2.H and T1.H vs T4.H anchored by thiol-yne
30 coupling chemistry. In all the cases, the concentration of probe was 1 μ M. For each chip
31 the experiment was the same, after flowing hybridization buffer (SSC 1 \times), Target B at 5
32 μ M was injected in both chips and flowed over for 25 min (Figure S6, Supporting
33 Information). After flowing buffer for several min, water was injected to dehybridize and
34 a non-complementary strand was later flowed in order to assess the specificity in the

1 hybridization. From the transverse electric (TE) and transverse magnetic (TM) plots,
2 quantitative data were extracted, as mass density, volume density, refractive index
3 variations, and layer thickness.

4 Considering the immobilization density obtained from the microarray assays for 1 μM
5 probe concentration, hybridization efficiencies were calculated in each case and
6 compared with those obtained in microarray format. Trends observed in these DPI
7 experiments were in agreement with the observed in microarrays. For thiol-ene coupling
8 approach, the density of hybridized oligonucleotide rose as the number of thiol moieties
9 in the probe increased. However, for thiol-yne immobilization, the hybridization
10 efficiency remained constant regardless the number of thiols present in the probe.
11 Interestingly, the same ratio of improvement in the hybridization efficiency was observed
12 for both microarray assays and DPI experiments in thiol-ene coupling and thiol-yne
13 coupling plots, when the number of thiols in the probes grew.

14 Using DPI, in thiol-ene coupling to move from one to two points attachment in the probe
15 increased the hybridization density 3.85-fold (in the case of microarray, it was 2.3-fold),
16 and to move from one to four thiols improved it 4.4-fold (3-fold for microarray). In the
17 case of thiol-yne immobilization, to change from one to two thiols raised the hybridization
18 density 1.24-fold (1.07-fold for microarray assays); and 1.4-fold more hybridization was
19 obtained when changing from one to four thiol groups (1.14-fold in the microarray). Thus,
20 using thiol-yne approach, the number of thiol moieties in the probe did not enhance
21 significantly the hybridization efficiency, as it was close to the maximal in all the cases.
22 On the contrary, the use of polythiolated probes is very adequate when working with
23 thiol-ene immobilization approach.

24 Regarding DPI data interpretation, the results pointed towards a tilted probe
25 immobilization, as was previously described,³² where the hybridization takes place also
26 in planar orientation. It is supported by the values of thickness increase and density
27 obtained after hybridization. As shown in Table 2, the thickness increase was very low
28 and nearly constant for all the cases, about 0.3 nm, whereas the density increased
29 considerably when mass was loaded on the surface by the effect of hybridization.

30

31 **Table 2:** DPI figures obtained for thiol-ene and thiol-yne coupling for T1.H, T2.H and T4.H after
32 hybridization with Target B 0.5 μM .

Thiol-ene			Thiol-yne		
T1.H	T2.H	T4.H	T1.H	T2.H	T4.H

Refractive Index	1.36	1.41	1.43	1.49	1.50	1.53
Thickness (nm)	0.33	0.34	0.29	0.28	0.32	0.39
Mass (ng/mm²)	0.04	0.14	0.15	0.24	0.30	0.42
Density (g/cm³)	0.11	0.42	0.53	0.87	0.94	1.06
Mass* (pmol/cm²)	0.50	1.89	2.16	3.37	4.18	5.87

*Calculated from the mass surface and considering a molecular weight for Target B of 7,127 g/mol

Considering the theoretical density of a double stranded DNA, 1.7 g/cm³, the obtained densities would correlate with the following percentages of dsDNA after hybridization having one, two and four thiol groups in the probe, respectively: 6%, 25% and 31% for thiol-ene coupling approach, and 51%, 55%, and 62% for thiol-yne strategy (Table 3).

Table 3: Probe immobilized density obtained from microarray assays, and hybridization efficiencies obtained in DPI experiments calculated considering the immobilized probe and the theoretical density of a double stranded DNA.

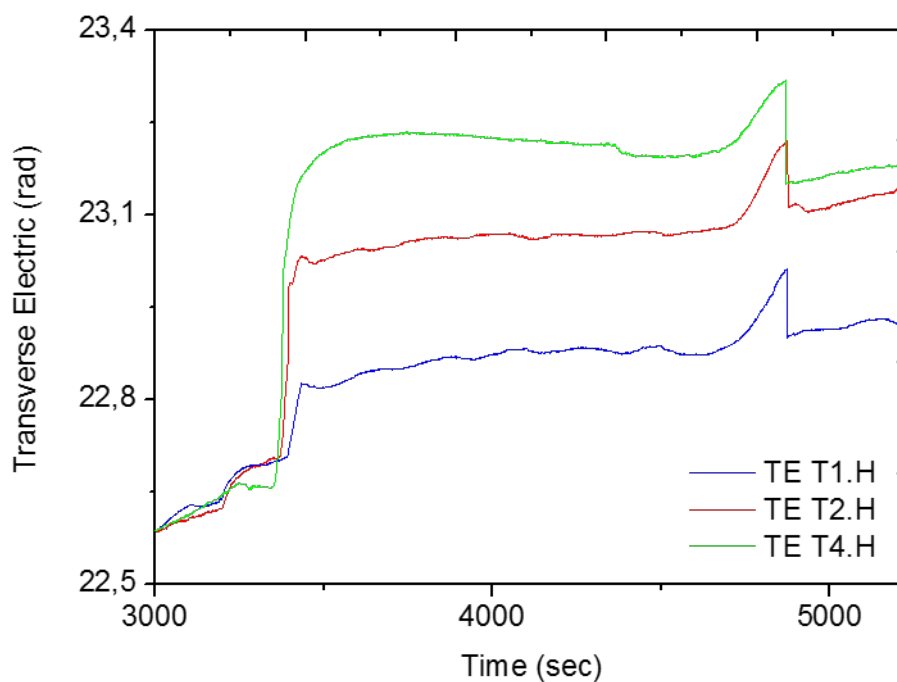
	Thiol-ene			Thiol-yne		
	T1.I	T2.I	T4.I	T1.I	T2.I	T4.I
Immobilized density (pmol/cm²)^a	8.08	12.6	13.11	22.9	23.3	25.5
Hybridization yield^b (%)	6	15	17	12	15	20
Hybridization yield^c (%)	6	25	31	51	55	62

^aMicroarray data for 1 μM of probe, ^bcalculated using the mass obtained in DPI, and the immobilized density determined by microarray ^ccalculated using the density obtained in DPI and the theoretical density of a double stranded DNA.

Nevertheless, taking into account that the amount of immobilized probe by thiol-ene coupling was half the immobilized probe reached by thiol-yne approach, we concluded that the four-thiol attachment enhances the performance in hybridization of thiol-ene coupling strategy, reaching the level of efficiency of thiol-yne coupling. This indicates that the control in the solid-probe-fluid interface can be done by using different surface chemistries, or by using probe multi-point attachment as well.

DPI experimental data suggest that the probes stand up in all cases for thiol-yne coupling attachment, while in the case of thiol-ene coupling attachment, the monothiolated probe lays down on the surface, and polythiolated probes stand up on the surface. This is determined by the theoretical thickness increase considering a perfect close packed dsDNA layer on the surface (when the surface coverage is less than 20%, the provided thickness is the averaged thickness, that is 0.20×Thickness dsDNA). Thus, when dividing the obtained experimental thickness by the hybridization percentage, the theoretical

1 thickness obtained resulted 2 nm for all cases, except for the case of thiol-ene coupled
2 monothiolated probe, whose thickness resulted 5.5 nm. This indicates that the probe, in
3 the last case has been straightened much more than in the other cases, which means that it
4 was much more tilted, laying down on the surface. This would difficult target
5 accessibility, diminishing then the hybridization capability.
6 It is worth noticing that DPI usually yields worse hybridization than microarray because
7 the incubation time is shorter, 25 min instead of 1 h, and the flow can negatively affect
8 the hybridization process.
9 In Figure 4, the Transverse Electric (TE) variation is plotted is shown for hybridization
10 of T1.H, T2.H and T4.H attached by thiol-ene coupling. The evolution of TE follows the
11 same trend in the three cases but the change in TE is bigger as the number of thiols in the
12 probe increases.



13
14 **Figure 4:** Transverse Electric evolution during hybridization of 0.5 μM of Target B in DPI for immobilized
15 probes T1.H, T2.H and T4.H (1 μM). Black arrows indicate the start and the end of the Target B injection
16 in the channels.
17

18 **PCR products detection**

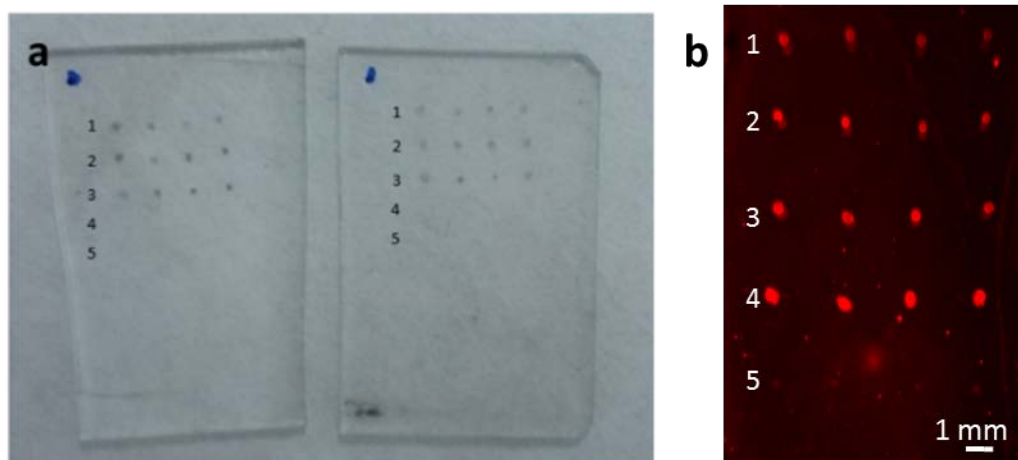
19 Finally, in order to demonstrate the applicability of the developments for real samples,
20 further experiments were done to detect PCR products of an innocuous specie of
21 *Salmonella*. In this case, glass was used as solid support instead of silica. The reason was

1 to assay colorimetric detection, which would allow naked eye identification without any
2 instrumental detection.

3 The functionalization proceeded in the same way as silica, as glass surfaces respond also
4 very well to organosilane functionalization. Three glass chips were functionalized with
5 vinyl triethoxysilane as before. Then each array was printed with the probes specific for
6 *Salmonella* T1.Sal, T2.Sal, and T4.Sal, containing one, two and four thiol groups,
7 respectively. Two sequences were also printed: the T1.I as immobilization control and
8 the T4.Cam targeting *Campylobacter* as a probe specificity control. Hybridization was
9 carried out for 1 h at 37 °C with a 1/10 dilution of the PCR products corresponding to a
10 500 pM concentration.

11 After hybridization with *Salmonella* digoxigenin-labeled PCR products, two chips were
12 incubated with a mixture containing anti-digoxigenin rabbit antibody (1/10000) and gold-
13 labeled goat anti-rabbit antibody (1/100). The microarrays were then developed with
14 silver enhancer solution, showing a black precipitate only in the rows corresponding to
15 T1.Sal, T2.Sal and T4.Sal (Figure 5a).

16



17

18 **Figure 5.** Microarrays on glass after hybridization with *Salmonella* PCR products. a) Colorimetric detection
19 using silver development format and b) Fluorescence detection. First row corresponds to T1.Sal, row 2
20 corresponds to T2.Sal, row 3 corresponds to T4.Sal, row 4 is T1.I, and row 5 corresponds to T4.Cam, both
21 controls.

22

23 The third chip was treated, after PCR products hybridization, with anti-digoxigenin rabbit
24 antibody (1/100) in PBS-T for 30 min, washed with water and incubated again with
25 Alexa647-labeled goat anti-rabbit antibody 1/50 in PBS-T for another 30 min. After
26 washing, the fluorescence was measured (Figure 5b). Fluorescence signal could be

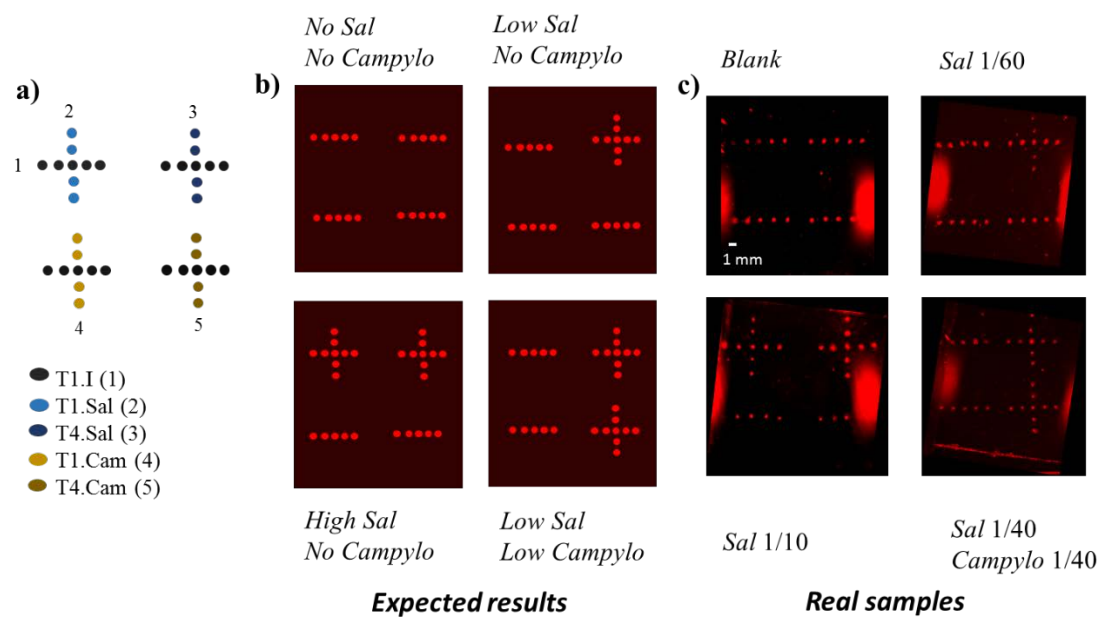
1 observed for the rows T1.Sal, T2.Sal and T4.Sal, and for control T1.I as well.
2 Fluorescence labelling allowed detection and quantification of the signal reached for each
3 probe. We observed that the dithiolated probe enhanced the signal 10% related to the
4 monothiolated T1.Sal, while tetrathiolated probe raised the signal up to 26% (Table S4,
5 Supporting Information). Although good sensitivity was obtained for all probes, it was
6 demonstrated again that multipoint probe attachment improved the hybridization
7 efficiency, even for large DNA fragments such the current PCR products (150 bp). In
8 addition, no hybridization was observed with the T4.Cam probe, demonstrating the
9 selectivity of the hybridization and the absence of non-specific immobilization on the
10 chip.

11 Using colorimetric detection, further experiments with more diluted PCR products (from
12 1/10 to 1/100) were done. Hybridization was detected up to dilution 1/40, which
13 corresponds to a concentration of 125 pM.

14 For dilutions below 1/40, only T4.Sal showed positive results. Thus, serial dilutions were
15 done and assayed for the tetrathiolated probe, in order to determine the lowest
16 concentration to be detected using the most sensitive probe (Figure S7, Supporting
17 Information). Under these conditions, the probe hybridized with dilutions up to 1/240,
18 which means a concentration of 20 pM. The selectivity of the probe of this concentration
19 level was assessed including a control row with a tetrathiolated probe specific for
20 *Campylobacter* bacteria. This probe didn't develop positive assay for *Salmonella* PCR
21 products but did for *Campylobacter* PCR products at 1/100.

22 As final demonstration of the applicability of the method proposed herein, a fluorescence-
23 based microarray assay was designed. In it T1.Sal, T4.Sal, T1.Cam, T4.Cam and T1.I
24 were immobilized as depicted in Figure 6a).

25



1
2 **Figure 6.** a) Scheme of the designed microarray where rows are printed with immobilization control probe
3 T1.I, whereas columns are printed with monothiolated (2) and tetrathiolated (3) probes for *Salmonella* and
4 monothiolated (4) and tetrathiolated (5) probes for *Campylobacter* (1 μ M) b) expected results for different
5 situations with low or high concentrations of bacterial DNA in samples c) obtained results for samples
6 without bacterial DNA (top-left), with low (top-right) and high (bottom-left) concentration of *Salmonella*'s
7 DNA and with a mixture of *Salmonella* and *Campylobacter* PCR products (bottom-right).

8
9 This design would allow easy differentiation of samples containing higher and lower
10 concentrations of *Salmonella*, and the same for *Campylobacter* (Figure 6b). These arrays
11 were prepared and assayed (by duplicate) with samples containing PCR products of
12 *Salmonella* and/or *Campylobacter* at different concentrations. The results obtained are
13 shown in Figure 6c, where two plus marks were obtained for *Salmonella* 1/10, while only
14 one plus mark was observed for dilution 1/60. The number and location of plus marks
15 indicated the bacteria specie present in the sample (*Salmonella*, *Campylobacter* or both)
16 and the concentration level (two plus marks for dilution up to 1/40, and only one mark
17 for higher dilutions).

18 CONCLUSION

19 In this work, thiol-ene and thiol-yne coupling chemistries have been evaluated to attach
20 mono and polythiolated probes onto alkenylated and alkynylated surfaces, respectively.
21 Studies tackled by dual polarization interferometry and on chip microarray fluorescence
22 format indicated that alkynyl terminated surfaces rendered higher immobilization yields
23 than thiol-ene linking. Polythiolated probes were more effectively immobilized on the

1 surface than the monothiolated ones. Closely related to the immobilized probe, the
2 hybridization density was also double in thiol-yne approach. However, it was observed
3 with the thiol-ene coupling chemistry that multipoint probe attachment improved
4 significantly the immobilization density and thus, the hybridization yield with the
5 complementary strand. This trend was also observed for thiol-yne coupling although less
6 pronounced. Also, for hybridization of large DNA strands, such as real bacterial PCR
7 products, the same behavior was noticed and detection was improved using multi-point
8 attachment in thiol-ene approach.

9 Consequently, there are two ways to improve the performance of a microarray; the first
10 one is to focus on the surface functionalization, tuning surface properties such as
11 hydrophobicity, and the second one is to control the surface-probe-fluid interface by
12 multi-point probe attachment. Both approaches seem to be closely related to the
13 configuration adopted by the attached probe, leading to its good availability for
14 hybridization with

15 PCR product. Considering these issues together when designing new microarrays could
16 help to reach advanced performance in the hybridization assays.

17 As demonstrated in the experiments, the created microarrays can be used with both
18 colorimetric and fluorescence detection techniques. The first provides higher sensitivity;
19 however, the second presents the advantages of lower number of steps and rapid readout.
20 The flexibility in the detection approach would allow the development of an assay where
21 the presence and concentration of bacterial DNA would be read by the naked eye.

22

23 **EXPERIMENTAL SECTION (Experimental Section has been moved behind** 24 **Conclusion section)**

25 **Chemicals, Reagents, and Buffers.** Silicon-based wafers were provided by Valencia
26 Nanophotonics Technology Center (NTC) at Universitat Politècnica de València (Spain)
27 from SIEGERT WAFER GmbH (Aachen, Germany) as a 2 mm thick silicon oxide layer
28 grown on a (1 0 0) silicon wafer. Glass microscope slides were obtained from Labbox
29 (Barcelona, Spain).

30 Allyltrimethoxysilane, vinyl trimethoxysilane, (3-glycidyloxypropyl)trimethoxysilane
31 (GOPTS), propargylamine, tris(2-carboxyethyl)phosphine hydrochloride (TCEP), and
32 silver developer solutions A and B were purchased from Sigma-Aldrich Química

1 (Madrid, Spain). Toluene, 2-propanol, and formamide were purchased from Scharlau
 2 (Madrid, Spain).

3 Oligonucleotide sequences Target A and Target B were acquired from Eurofins
 4 Genomics (Ebersberg, Germany). Monothiolated oligonucleotide sequences T1.I, T1.H
 5 and T1.Cam were acquired from Aldrich Quimica (Madrid, Spain).

6 Polythiolated-modified probes T2.I, T4.I, T2.H, T4.H, T1.Sal, T2.Sal, T4.Sal, T4.Cam
 7 (Table 4) were synthesized on a 1 μ mol-scale by standard phosphoramidite chemistry
 8 using a 394 ABI DNA synthesizer. Cy5 solid support was purchased from Link
 9 Technologies (Lanarkshire, Scotland). For the coupling step, benzylmercaptotetrazole
 10 (BMT) was used as the activator (0.3 M in anhydrous CH₃CN) along with commercially
 11 available nucleoside phosphoramidites (dT, dABz, dCBz and dGtBuPac) at 0.075 M in
 12 anhydrous CH₃CN introduced with a 20 s coupling time, 1-O-(4,4'-dimethoxytrityl)-2-(6-
 13 S-acetylthio hexyl oxymethyl)-2-methyl-3-(diisopropylamino β -cyanoethyl
 14 phosphoramidite)-propane-1,3-diol^[27] now commercially available from Chemgenes
 15 Corporation (0.1 M in anhydrous CH₃CN) with a 60 s coupling time. The capping step
 16 was performed with phenoxyacetic anhydride using commercial solutions (Cap A: Pac₂O,
 17 pyridine, THF 10/10/80 and Cap B: 10% N-methylimidazole in THF) for 60 s. Oxidation
 18 was performed with a commercial solution of iodide (0.1 M I₂, THF/pyridine/water
 19 90/5/5) for 13 s. Detritylation was performed with 3% TCA in CH₂Cl₂ for 65 s.

20 **Table 4.** Oligonucleotide sequences list, including functionalities.

Name	Sequence (5' to 3')	5' end	3' end
T1.I	CCCGATTGACCAGCTAGCATT	1 SH	Cy5
T2.I	CCCGATTGACCAGCTAGCATT	2 SH	Cy5
T4.I	CCCGATTGACCAGCTAGCATT	4 SH	Cy5
T1.H	CCCGATTGACCAGCTAGCATT	1 SH	
T2.H	CCCGATTGACCAGCTAGCATT	2 SH	
T4.H	CCCGATTGACCAGCTAGCATT	4 SH	
Target A	AATGCTAGCTGGTCAATCGGG	Cy5	
Target B	AATGCTAGCTGGTCAATCGGG		
T1.Sal	T4GATTACAGCCGGTGTACGACCCT	1 SH	
T2.Sal	T4GATTACAGCCGGTGTACGACCCT	2 SH	
T4.Sal	T4GATTACAGCCGGTGTACGACCCT	4 SH	
T1.Cam	T4AGACGCAATACCGCGAGGTGGAGCA	1 SH	
T4.Cam	T4AGACGCAATACCGCGAGGTGGAGCA	4 SH	

21

1 **Protocol for deprotection.** After elongation, the solid-supported S-acetylthiol-
2 oligonucleotides were treated with a solution of 10% piperidine in dry CH₃CN in a
3 continuous flow manner (5 mL over 15 min), before being washed with dry CH₃CN and
4 dried using a flush of nitrogen. Then, solid-supported thiolated oligonucleotides were
5 treated with concentrated ammonia for 2 h at room temperature. The filtrate was
6 withdrawn and evaporated affording the polythiolated probes. The residue was dissolved
7 in 1 mL of water and washed three times with ethyl acetate to remove benzamide and
8 tert-butylphenoxyacetamide. After MALDI-TOF characterization (Table S1), the crude
9 modified oligonucleotides were lyophilized and stored at -20°C. The structure of the
10 thiolated probes can be seen in Figure S1 (Supporting Information)

11 Milli-Q water 18 mΩ was used to prepare aqueous solutions. The buffers employed,
12 phosphate buffer saline (PBS 1×, 0.008M sodium phosphate dibasic, 0.002 M sodium
13 phosphate monobasic, 0.137 M sodium chloride, 0.003 M potassium chloride, pH 7.5),
14 PBS-T (PBS 10× containing 0.05% Tween 20), saline sodium citrate (SSC 10×, 0.9 M
15 sodium chloride, 0.09 M sodium citrate, pH 7) and washing solutions were filtered
16 through a 0.22 μm pore size nitrocellulose membrane from Whatman GmbH (Dassel,
17 Germany) before use.

18 Digoxigenin-labeled PCR products from *Salmonella* were obtained in the laboratory, as
19 previously described,^[35,36] with a concentration of 546.38 ng/ml (5 nM) determined by
20 fluorescence.

21 Anti-digoxigenin recombinant monoclonal antibody from rabbit and goat anti-rabbit
22 Alexa Fluor 647 antibody were purchased from Invitrogen Life Technologies (Carlsbad,
23 CA). Gold labeled goat anti-rabbit was ordered from Sigma-Aldrich (Madrid, Spain).

24 **Instrumental methods.** Surface activation was carried out with a UV-Ozone cleaning
25 system UVOH150 LAB (FHR, Ottendorf-Okrilla, Germany).

26 Microarrays were printed with a low volume noncontact dispensing system from Biodot
27 (Irvine, CA), model AD1500.

28 Probe photoattachment was done with a mercury capillary lamp Jelight (6 mW/cm²,
29 Jelight Irvine, CA).

30 Contact angle measurements were carried out with Dino-Lite Microscope and image
31 treated with Dino Capture software (Torrance, CA). The measurements were done in
32 triplicate at room temperature with a volume drop of 5 μl employing 18 mΩ water quality.

33 The fluorescence signal of the spots in the microarrays was registered with a homemade
34 surface fluorescence reader (SFR),³⁷ having a high sensitivity charge coupled device

1 camera Retiga EXi from Qimaging, Inc. (Burnaby, Canada), with light emitting diodes
2 Toshiba TLOH157P as light source. Microarray image treatment and quantification was
3 done using GenePix Pro 4.0 software from Molecular Devices, Inc. (Sunnyvale, CA).
4 Dual Polarization Interferometry studies were carried out with an Analight2000 device
5 (Biolin Scientific, Stockholm, Sweden). Raw silicon oxynitride Anachips (Biolin
6 Scientific) were employed and biofunctionalized as required in each case.
7 MALDI-ToF mass spectra were registered on a Voyager mass spectrometer (Perspective
8 Biosystems, Framingham, MA) equipped with a nitrogen laser. MALDI conditions were:
9 accelerating voltage 24000V; guide wire 0.05% of the accelerating voltage; grid voltage
10 94% of the accelerating voltage; delay extraction time 700 ns. 1 μ L of sample was mixed
11 with 5 μ L of a saturated solution of THAP in acetonitrile/water (1:1, v/v) containing 10%
12 of ammonium citrate and few beads of DOWEX 50W-X8 ammonium sulfonic acid resin
13 were added. Then, 1 μ L of the mixture was placed on a plate and dried at room
14 temperature and pressure.
15 X-ray photoelectron spectra were recorded with a Sage 150 spectrophotometer from
16 SPECS Surface Nano Analysis GmbH (Berlin, Germany). Non-monochromatic Al K α
17 radiation (1486.6 eV) was used as the X-ray source operating at 30 eV constant pass
18 energy for elemental specific energy binding analysis. Vacuum in the spectrometer
19 chamber was 9×10^{-9} hPa and the sample area analyzed was 1 mm². Atomic Force
20 Microscopy (AFM) measurements were carried out with a Veeco model Dimension 3100
21 Nanoman from Veeco Metrology, (Santa Barbara, CA) using tapping mode at 300 kHz.
22 Imaging was performed in AC mode in air using OMCL-AC240 silicon cantilevers
23 (Olympus Corporation, Japan). The images were captured using tips from Nano World
24 with a radius of 8 nm. All AFM images were processed with WSxM software.³⁸

25

26 **Surface chemical modification.** Silicon wafers were cut into pieces of 2 x 1 cm², cleaned
27 with water first, then with 2-propanol and blow dried. Afterwards, they were placed in
28 the UV-ozone cleaner, and irradiated for 7 min. The chips were functionalized
29 immediately after activation.

30 For alkenylation, activated chips were introduced into a solution of vinyltrimethoxy silane
31 (2% v/v in toluene) for 2 h at room temperature. The chips were cleaned with toluene,
32 then with 2-propanol, and blow dried with compressed air. Then they were baked at
33 150 °C in an oven for 30 min.

1 To introduce the alkynyl groups, the chips were immersed under argon atmosphere into
2 a solution of (3-glycidioxypropyl)trimethoxysilane (GOPTS) 2% in toluene for 2 h at
3 room temperature. After 2 h, the chips were washed with 2-propanol and air-dried. Next,
4 the chips were baked for 30 min at 150 °C and after cooling at room temperature, they
5 were immersed in a solution of propargylamine 2% in toluene for 4 h. Finally, the chips
6 were washed with 2-propanol, air-dried, and baked for 30 min at 150 °C.

7 **Probe immobilization studies.** To perform this study, solutions of oligonucleotides T1.I,
8 T2.I and T4.I at 2, 1 and 0.5 µM were prepared in PBS 1× from a starting concentration
9 of 20 µM (50 µl of oligonucleotide 100 µM, 150 µl MilliQ water and 50 µl of TCEP
10 0.1M in MilliQ water).

11 These solutions were spotted (40 nl/spot, humidity set at 95%) onto the functionalized
12 surfaces creating microarrays where each row contained 5 replicas (spots); the number of
13 rows was nine (one row per oligo and concentration).

14 The microarrays were then exposed to UV-light at 365 nm, with the lamp placed at a
15 fixed distance (5 cm) from the slide, for 60 min to induce the immobilization (mono or
16 multipoint attachment). Finally, slides were thoroughly rinsed with water and air-dried.
17 By the SFR, fluorescence measurements let us to quantify the immobilization yield.
18 Measurements were made by accumulation of emitted light by the samples during 15
19 seconds with a device gain of 3.

20 **Hybridization studies.** Solutions of oligonucleotides T1.H, T2.H and T4.H 0.1, 0.2, 0.4,
21 0.5 1, 2, 3 and 5 µM were prepared in PBS 1× from a starting concentration of 20 µM.
22 For each type of oligonucleotide, a microarray was printed on a functionalized surface (5
23 spots/row, 40 nl/spot, 8 rows, humidity set at 95%) using the robotic arrayer. The slides
24 were then irradiated as before, rinsed with water, and air dried. Afterwards, 50 µl of
25 Target A (0.5 µM in SSC 1×) were spread over the entire surface with a coverslip. After
26 incubation in a slim box for 45 min at 37 °C, the coverslip was gently removed and the
27 chip washed with SSC 0.1× and air dried. The fluorescence intensity of the spots was
28 registered with the SFR as described above.

29 **Salmonella PCR products detection.** Glass slides were cut in 2 x 1 cm² pieces and
30 activated and functionalized with alkene groups as described above for silicon surfaces.
31 Then microarrays of probes T1.Sal, T2.Sal, T4.Sal at 2 µM in PBS1×, T1.I as
32 immobilization control, and T4.Cam as non-specific hybridization control (both at 2 µM),
33 were printed and immobilized as described before.

1 After irradiation, washing and drying, the chips were ready for hybridization. Firstly, they
2 were pre-hybridized in SSC 1×, 15% formamide, at 37 °C for 30 min. Then, 35 µl of PCR
3 product (dilutions ranging from 1/10 to 1/100) in SSC 1×, 15% formamide, were
4 dispensed on the chips and spread out over the surface using a coverslip. The target PCR
5 products were denaturalized at 95 °C for 5 min and then cooled down in ice for 2 min
6 immediately before the hybridization. The chips were incubated at 37 °C for 60 min, then
7 washed with SSC 0.1× and air dried.

8 For naked-eye detection, a mixture containing rabbit anti-digoxigenin antibody (1/10000)
9 and gold labeled goat anti-rabbit antibody (1/100) in PBS-T were applied over the chip,
10 and incubated for 30 min at room temperature. After washing with PBS-T, the chips were
11 incubated with 20 µl of silver developer solution, and after 12 min, positive results (silver
12 deposition) appeared on the microarrays.

13 For fluorescence detection and quantification, 30 µl of anti-digoxigenin antibody
14 produced in rabbit, 1/100 in PBS-T, were spread over the chip and incubated for 30 min
15 at room temperature. After washing with PBS-T, 30 µl of Alexa647-labeled goat anti-
16 rabbit antibody, 1/50 in PBS-T, were incubated over the chip for another 30 min at room
17 temperature. Finally, the chip was washed with PBS-T, water and air dried, and the
18 fluorescence registered with the SFR.

19 **DPI hybridization experiments.** Unmodified Anachips were functionalized with
20 alkenyl or alkynyl groups as described before. One of the channels was used to
21 immobilize T1.H, while the other channel was employed to attach T2.H in one case, and
22 T4.H in the other case. The spatial selectivity for the probe tethering only on one of the
23 two channels available was achieved by selective irradiation using a homemade
24 photomask. The chip was inserted in the device, and calibrated following fabricant
25 instructions. The carrier buffer was SSC 1×. Target B 5 µM in SSC 1× was flowed over
26 both channels for 25 min at a flow rate of 10 µl/min. Afterwards, water (25 min, 10
27 µl/min) was injected to dehybridize. Then, a non-complementary strand (25 µM, 10
28 µl/min, 5 min) was flowed to assess the specificity of the recognition.

29

30 **ASSOCIATED CONTENT**

31 **Supporting Information**

32 MALDI-TOF MS of oligonucleotides, Contact angle values, Calculated Immobilization
33 densities, Calibration curve for Target A, AFM Surface characterization, XPS C1s peak

1 deconvolution of alkene-ended biofunctionalized surfaces, Data obtained by DPI, Results
2 for a colorimetric microarray. This material is available free of charge via the Internet at
3 <http://pubs.acs.org>.

4

5 **AUTHOR INFORMATION**

6 **Corresponding Author**

7 *Phone: 34-963873415; fax: 34-963879349; E-mail: amaqueira@quim.upv.es

8 *Phone: 33-(0)-467144961; fax: 33-(0)-467042029; E-mail:

9 francois.morvan@umontpellier.fr

10

11 **Notes**

12 The authors declare no competing financial interest.

13

14 **ACKNOWLEDGMENTS**

15 The authors thank Dr. Elena Pinilla for her helpful discussion about AFM results.

16 This work was funded by EU's program Horizon 2020 ICT-26-2014-644242, Spanish
17 Ministry MINECO CTQ/2013/45875-R FEDER and local administration GVA
18 PROMETEO II 2014/40. The authors acknowledge Tortajada-Genaro, Luis and Niños
19 Rodenes, Regina for kindly providing the *Salmonella* and *Campylobacter* PCR products.
20 F.M. is member of Inserm.

21

22 **Abbreviations**

23 GOPTS: (3-glycidylxypropyl)trimethoxysilane, TCEP: tris(2-carboxyethyl)phosphine
24 hydrochloride, THF: tetrahydrofurane, TCA: trichloroacetic acid, PBS: Phosphate buffer
25 saline, SSC: sodium citrate saline buffer, SFR: surface fluorescence reader, DPI: Dual
26 polarization , Interferometry, RSD: Relative standard desviation, , AFM: Atomic Force
27 microscopy, XPS: X-ray photoelectron spectroscopy, TE: Transverse electrical, TM:
28 Transverse magnetical, dsDNA: double strand DNA

29 **REFERENCES**

30 (1) Huys, I., Matthijs, G., and Van Overwalle, G. (2012) The fate and future of patents

- 1 on human genes and genetic diagnostic methods. *Nat. Rev. Genet.* *13*, 441–8.
- 2 (2) Sett, A., Das, S., and Bora, U. (2014) Functional nucleic-acid-based sensors for
3 environmental monitoring. *Appl. Biochem. Biotechnol.* *174*, 1073–91.
- 4 (3) Sett, A. (2012) Aptasensors in Health, Environment and Food Safety Monitoring.
5 *Open J. Appl. Biosens.* *1*, 9–19.
- 6 (4) Scheler, O., Glynn, B., and Kurg, A. (2014) Nucleic acid detection technologies and
7 marker molecules in bacterial diagnostics. *Expert Rev. Mol. Diagn.* *14*, 489–500.
- 8 (5) Sassolas, A., Leca-Bouvier, B. D., and Blum, L. J. (2008) DNA biosensors and
9 microarrays. *Chem. Rev.* *108*, 109–139.
- 10 (6) Ji, H., and Davis, R. W. (2006) Data quality in genomics and microarrays. *Nat.*
11 *Biotechnol.* *24*, 1112–1113.
- 12 (7) Rao, A. N., and Grainger, D. W. (2014) Biophysical properties of nucleic acids at
13 surfaces relevant to microarray performance. *Biomater. Sci.* *2*, 436.
- 14 (8) Heller, M. J. (2002) DNA Microarray Technology: Devices, Systems, and
15 Applications. *Annu. Rev. Biomed. Eng.* *4*, 129–153.
- 16 (9) Barbulovic-Nad, I., Lucente, M., Sun, Y., Zhang, M., Wheeler, A. R., and
17 Bussmann, M. (2006) Bio-Microarray Fabrication Techniques—A Review. *Crit. Rev.*
18 *Biotechnol.* *26*, 237–259.
- 19 (10) Wu, P., Castner, D. G., and Grainger, D. W. (2008) Diagnostic devices as
20 biomaterials: a review of nucleic acid and protein microarray surface performance
21 issues. *J. Biomater. Sci. Polym. Ed.* *19*, 725–53.
- 22 (11) Zhou, X. C., Huang, L. Q., and Li, S. F. Y. (2001) Microgravimetric DNA sensor
23 based on quartz crystal microbalance: comparison of oligonucleotide immobilization
24 methods and the application in genetic diagnosis. *Biosens. Bioelectron.* *16*, 85–95.
- 25 (12) Pan, S., and Rothberg, L. (2005) Chemical Control of Electrode Functionalization
26 for Detection of DNA Hybridization by Electrochemical Impedance Spectroscopy.
27 *Langmuir* *21*, 1022–1027.
- 28 (13) Manning, B., and Eritja, R. (2012) Functionalization of Surfaces with Synthetic

- 1 Oligonucleotides, Melba Navarro and Josep A. Planell (eds.), *Nanotechnology in*
2 *Regenerative Medicine: Methods and Protocols, Methods in Molecular Biology*, 811,
3 89–100.
- 4 (14) Singh, V., Zharnikov, M., Gulino, A., and Gupta, T. (2011) DNA immobilization,
5 delivery and cleavage on solid supports. *J. Mater. Chem.* 21, 10602.
- 6 (15) Nimse, S., Song, K., Sonawane, M., Sayyed, D., and Kim, T. (2014)
7 Immobilization Techniques for Microarray: Challenges and Applications. *Sensors* 14,
8 22208–22229.
- 9 (16) Kolb, H. C., Finn, M. G., and Sharpless, K. B. (2001) Click chemistry Diverse
10 chemical function from a few good reactions. *Angew. Chemie - Int. Ed.* 40, 2004–2021.
- 11 (17) Hoyle, C. E., and Bowman, C. N. (2010) Thiol-ene click chemistry. *Angew.*
12 *Chemie - Int. Ed.* 49, 1540–1573.
- 13 (18) Dondoni, A. (2008) The emergence of thiol-ene coupling as a click process for
14 materials and bioorganic chemistry. *Angew. Chemie - Int. Ed.* 47, 8995–8997.
- 15 (19) Massi, A., and Nanni, D. (2012) Thiol-yne coupling: revisiting old concepts as a
16 breakthrough for up-to-date applications. *Org. Biomol. Chem.* 10, 3791.
- 17 (20) Hoogenboom, R. (2010) Thiol-yne chemistry: A powerful tool for creating highly
18 functional materials. *Angew. Chemie - Int. Ed.* 49, 3415–3417.
- 19 (21) Wendeln, C., Rinnen, S., Schulz, C., Arlinghaus, H. F., and Ravoo, B. J. (2010)
20 Photochemical microcontact printing by thiol-ene and thiol-yne click chemistry.
21 *Langmuir* 26, 15966–15971.
- 22 (22) Campos, M. a C., Paulusse, J. M. J., and Zuilhof, H. (2010) Functional monolayers
23 on oxide-free silicon surfaces via thiol-ene click chemistry. *Chem. Commun.* 46, 5512–
24 5514.
- 25 (23) Mehlich, J., and Ravoo, B. J. (2011) Click chemistry by microcontact printing on
26 self-assembled monolayers: a structure-reactivity study by fluorescence microscopy.
27 *Org. Biomol. Chem.* 9, 4108–4115.
- 28 (24) Bertin, A., and Schlaad, H. (2009) Mild and Versatile (Bio-)Functionalization of
29 Glass Surfaces via Thiol-Ene Photochemistry. *Chem. Mater.* 21, 5698–5700.

- 1 (25) Iwasaki, Y., and Ota, T. (2011) Efficient biotinylation of methacryloyl-
2 functionalized nonadherent cells for formation of cell microarrays. *Chem. Commun.*
3 *(Camb)*. 47, 10329–10331.
- 4 (26) Wendeln, C., Rinnen, S., Schulz, C., Kaufmann, T., Arlinghaus, H. F., and Ravoo,
5 B. J. (2012) Rapid preparation of multifunctional surfaces for orthogonal ligation by
6 microcontact chemistry. *Chem. - A Eur. J.* 18, 5880–5888.
- 7 (27) Jonkheijm, P., Weinrich, D., Köhn, M., Engelkamp, H., Christianen, P. C. M.,
8 Kuhlmann, J., Maan, J. C., Nüsse, D., Schroeder, H., Wacker, R., et al. (2008)
9 Photochemical surface patterning by the thiol-ene reaction. *Angew. Chemie - Int. Ed.*
10 47, 4421–4424.
- 11 (28) Weinrich, D., Köhn, M., Jonkheijm, P., Westerlind, U., Dehmelt, L., Engelkamp,
12 H., Christianen, P. C. M., Kuhlmann, J., Maan, J. C., Nüsse, D., et al. (2010)
13 Preparation of biomolecule microstructures and microarrays by thiol-ene
14 photoimmobilization. *ChemBioChem* 11, 235–247.
- 15 (29) Weinrich, D., Lin, P. C., Jonkheijm, P., Nguyen, U. T. T., Schröder, H., Niemeyer,
16 C. M., Alexandrov, K., Goody, R., and Waldmann, H. (2010) Oriented immobilization
17 of farnesylated proteins by the thiol-ene reaction. *Angew. Chemie - Int. Ed.* 49, 1252–
18 1257.
- 19 (30) Lin, P. C., Weinrich, D., and Waldmann, H. (2010) Protein biochips: Oriented
20 surface immobilization of proteins. *Macromol. Chem. Phys.* 211, 136–144.
- 21 (31) Escorihuela, J., Bañuls, M. J., Puchades, R., and Maquieira, Á. (2012) DNA
22 microarrays on silicon surfaces through thiol-ene chemistry. *Chem. Commun.* 48, 2116.
- 23 (32) Escorihuela, J., Bañuls, M. J., Grijalvo, S., Eritja, R., Puchades, R., and Maquieira,
24 Á. (2014) Direct covalent attachment of DNA microarrays by rapid thiol-ene “click”
25 chemistry. *Bioconjug. Chem.* 25, 618–627.
- 26 (33) Escorihuela, J., Bañuls, M.-J., Puchades, R., and Maquieira, Á. (2014) Site-specific
27 immobilization of DNA on silicon surfaces by using the thiol–yne reaction. *J. Mater.*
28 *Chem. B* 2, 8510–8517.
- 29 (34) Lereau, M., Fournier-Wirth, C., Mayen, J., Farre, C., Meyer, A., Dugas, V.,
30 Cantaloube, J. F., Chaix, C., Vasseur, J. J., and Morvan, F. (2013) Development of

- 1 innovative and versatile polythiol probes for use on elosa or electrochemical biosensors:
2 Application in hepatitis c virus genotyping. *Anal. Chem.* 85, 9204–9212.
- 3 (35) Arnandis-Chover, T., Morais, S., Tortajada-Genaro, L. a., Puchades, R., Maquieira,
4 a., Berganza, J., and Olabarria, G. (2012) Detection of food-borne pathogens with DNA
5 arrays on disk. *Talanta* 101, 405–412.
- 6 (36) Santiago-Felipe, S., Tortajada-Genaro, L. A., Morais, S., Puchades, R., and
7 Maquieira, Á. (2015) Isothermal DNA amplification strategies for duplex
8 microorganism detection. *Food Chem.* 174, 509–515.
- 9 (37) Mira, D., Llorente, R., Morais, S., Puchades, R., Maquieira, A., and Marti, J.
10 (2004) High-throughput screening of surface-enhanced fluorescence on industrial
11 standard digital recording media, in *European Symposium on Optics and Photonics for*
12 *Defence and Security* (Carrano, J. C., and Zukauskas, A., Eds.), pp 364–373.
13 International Society for Optics and Photonics.
- 14 (38) Horcas, I., Fernández, R., Gómez-Rodríguez, J. M., Colchero, J., Gómez-Herrero,
15 J., Baro, A. M. (2007) WSXM: A Software for Scanning Probe Microscopy and a Tool
16 for Nanotechnology. *Rev. Sci. Instrum.* 78, 013705–8.

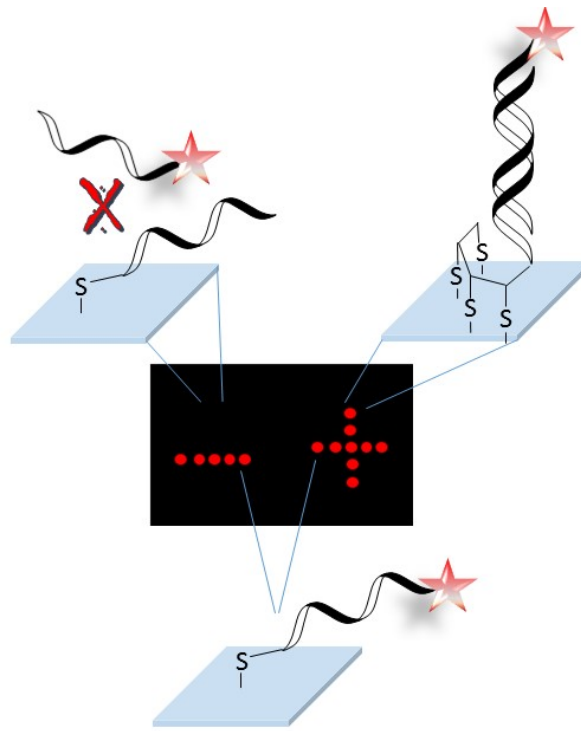
17

18

19

20

- 1 TOC
- 2 Controlling the solid-probe-fluid interface by probe multi-point attachment improves significantly
- 3 the hybridization process



- 4
- 5